ACS OMEGA

http://pubs.acs.org/journal/acsodf

Article

Dealkalization and Leaching Behavior of Fe, Al, Ca, and Si of Red Mud by Waste Acid from Titanium White Production

Zhanghao Jiang, Xuejun Quan,* Shuai Zhao, Kui Zeng, Hao Chen, and Yankuo Zhou

Cite This: *ACS Omega* 2021, 6, 32798−32808

Read Online

ACCESS | Metrics & More | Article Recommendations | Supporting Information

ABSTRACT: Dealkalization is the necessary step for the multipurpose use of red mud (RM), and acid leaching is a productive method to realize the dealkalization of RM. Most researches focus on recovering metals from the highly alkaline waste by pure acid leaching or stabilization by dealkalization. In this study, according to the strong alkalinity of RM and strong acidity of the waste acid from titanium dioxide production, the waste acid was used for the dealkalization of RM. The effects of leaching temperature, reaction time, the concentration of waste acid, liquid−solid ratio (L/S), and stirring rate on the dealkalization of RM were investigated, and the main metal ions in the dealkalization solution were analyzed. The results show that the leaching ratio of sodium can reach 92.3591% when the leaching temperature is 30 °C, the reaction time is 10 min, the concentration of waste acid is 0.6238 mol/L, the L/S is 4:1, and the stirring rate is 300 rpm. The residual alkali content in the treated RM is 0.2674%, which is a reduction to less than 1%. The phase analysis results show that the sodalite and cancrinite in RM are dissolved, decomposed, and transformed after acid leaching. Therefore, RM meets the requirements of building materials after dealkalization, which provides further development as building material products.

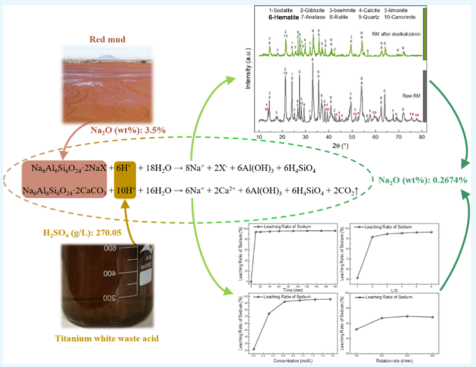

1. INTRODUCTION

Red mud (RM) is a high alkaline industrial solid noxious waste produced from the extraction of alumina from bauxite. It is called RM because it contains iron oxide and looks similar to the red soil.[1] In addition, its long-term storage poses a potential threat to the environment. With the rapid development of the alumina industry, the strong alkalinity of RM has become a bottleneck restricting the sustainable development of the global aluminum industry. According to the characteristics of bauxites and process conditions, every ton of alumina produced produces about 1−2.5 tons of RM.[2] This leads to global production of 100−150 million tonnes per year of RM.[3] Currently, the total utilization rate of RM in the world is about 15%, while it is only 5% in China.[4] Dam stacking is the leading way to dispose of RM.[5,6] RM is often pumped into storage tanks through wet treatment technology or stored in large quantities through dry or semi-dry methods.[7−9] However, many alkaline substances in red mud cause severe pollution to soil and water resources.[10−14] The leachate of the RM storage site contains many alkaline substances, which pollute the surrounding soil and water and cause various environmental problems.[15−18] In addition, RM can cause dust hazards to the surrounding community and the ecological environment in the downwind area because of its fine particle size.[19,20] Therefore, the effective utilization and harmless treatment of RM have attracted much attention.

RM can be used as adsorption materials, soil clusters, construction materials, catalytic materials, and recovery of precious metals.[21] Among them, soil aggregates and building materials can consume a large amount of RM, significantly reducing the environmental pollution.[22] Therefore, RM is used to form soil aggregates and building materials, which is very important for the large-scale recycling of RM. However, the application of RM in soil aggregates and building materials is limited by its high alkalinity.[23] Only when RM is neutral or weak alkaline can it be used as a soil aggregate.[23] Furthermore, the sodium content of RM applied to building materials must be less than 1% to prevent frost from damaging the quality of building materials.[24] However, the raw RM cannot be directly used as soil aggregates or building materials because its sodium content reaches 6−10%.[25] Therefore, it is necessary to reduce the alkalinity of RM before application.

Dealkalization methods for RM include water leaching, acid leaching, wet carbonization, and calcium ion replacement.[26−28] Quadruple water direct leaching method only removes free alkali in RM, and the leaching ratio of sodium is less than 71%.[29] Because the water leaching process does not consume additional reagents, it is economical. Still, this process is time-consuming because long-term leaching and repeated dealkalization are necessary for the water leaching process.[29] Therefore, the comprehensive utilization of the RM water leaching dealkaliza-

Received: August 29, 2021
Accepted: November 15, 2021
Published: November 25, 2021

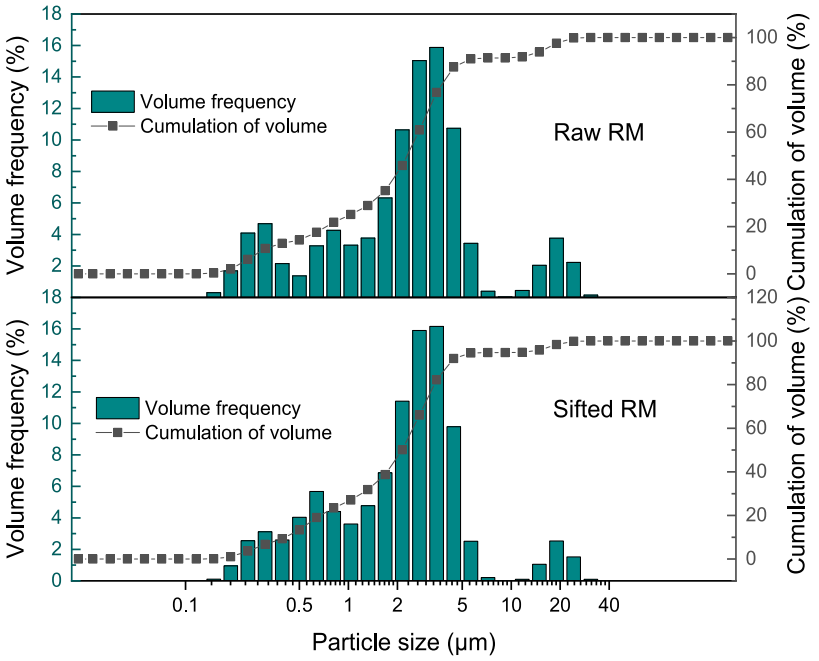

Figure 1. Particle size distribution map of RM before and after screening with 100 mesh.

tion method is limited.[29] The leaching ratio of sodium of the calcium ion replacement method is less than 80%. This method removes free alkali and structural alkali in RM, slightly higher than the water immersion method. However, this method needs to consume many reagents, so it is of low economic type.[30,31] The sodium removal efficiency of wet carbonization is generally less than 85%. This method can effectively remove free alkali and structural alkali in RM without consuming additional chemical reagents. However, wet carbonization requires high pressure and strict requirements for leaching equipment, so it is low in the economy.[32,33] Acid neutralization is the easiest way to achieve dealkalization because it is the most straightforward chemical reaction. It is generally believed that the higher the acid concentration, the higher the dissolution efficiency of alkali. Due to its strong acidity, the hydroxide, carbonate, and even oxide in RM may react with acid and be leached.[22,34] Chen et al. reported that the dissolution efficiency of sodium was improved at a higher H_2SO_4 concentration, and the dissolution efficiency of sodium reached 99.99% at 20°C, 1.8 mol/L H_2SO_4, and 30 min reaction time.[35]

The study mainly focused on the strong acid treatment of RM and recovery of leached metal[36−38] but ignored the alkali reduction and stability of RM at low acid concentrations. In this paper, the use of industrial waste acid solution to reduce the alkali of RM at a low temperature can effectively reduce the alkaline of RM and solve the main limiting factors of its comprehensive utilization. Furthermore, the acidic industrial wastewater was treated to achieve the comprehensive utilization of waste.

2. RESULTS AND DISCUSSION

2.1. Particle Size Analysis. The dried RM was screened according to 100 mesh, and the particle size of RM before and after the screening was further compared to make the particle size of RM used in the experiment consistent. Figure 1 and Table S1 show the particle size distribution of RM before and after screening with 100 mesh. It can be seen that the particle size of 0.010−2.584 μm is more than 50% of the maximum volume, and the raw RM particle size is mainly between 0.1 and 6 μm. The particle size distribution of RM was almost identical to RM before and after screening with 100 mesh. Therefore, it further explains the fine particle size of RM itself.[39] RM can be directly used for the leaching of waste acid to reduce alkali without pregrinding.

2.2. Leaching Behaviors of RM. *2.2.1. Effect of Temperature.* The samples were leached by the waste acid concentration of 1.2448 mol/L at different temperatures for 120 min, with a stirring speed of 300 rpm and a liquid−solid ratio (L/S) of 4/1 (mL/g). The effects of diverse temperatures on sodium, silicon, calcium, aluminum, and iron leaching are shown in Figure 2.

The leaching ratio of sodium in acid leached RM is more than 93%, as shown in Figure 2a. With the increase in temperature from 30 to 70 °C, the leaching ratio of sodium increased from 93.838 to 96.162%, and the rising trend was not noticeable. The leaching ratio of sodium aluminosilicate and other alkaline substances increased with the increase in temperature in RM, and the leaching balance of sodium gradually shifted to the right as shown in the chemical reaction (1),[40] which eventually led to the gradual accumulation of alkali leaching ratio. However, the leaching ratio of sodium only increases by 0.5% with every 10 °C increase in temperature in RM. As shown in Figure 2b−e, with the increase in temperature, the concentration of aluminum, calcium, iron, and silicon ions in the acid leaching solution showed a decreasing trend. As the reaction temperature increases and the alkaline substances are further released in RM, the aluminum and iron ion concentrations decrease with the increase in the pH value.[41] Simultaneously, silicon ions can be polymerized in the form of silicic acid and co-precipitate with aluminum, iron, and calcium ions,[42] which are eventually separated in the solid−liquid separation process, ultimately leading to the reduced concentrations of Fe, Al, Ca, and Si in the solution.[43] The possible reaction formulas are shown in eqs 1−7.[40,44] Therefore, 30 °C was selected as the optimal temperature of the dealkalization of RM in this experiment.

https://doi.org/10.1021/acsomega.1c04713
ACS Omega 2021, 6, 32798−32808

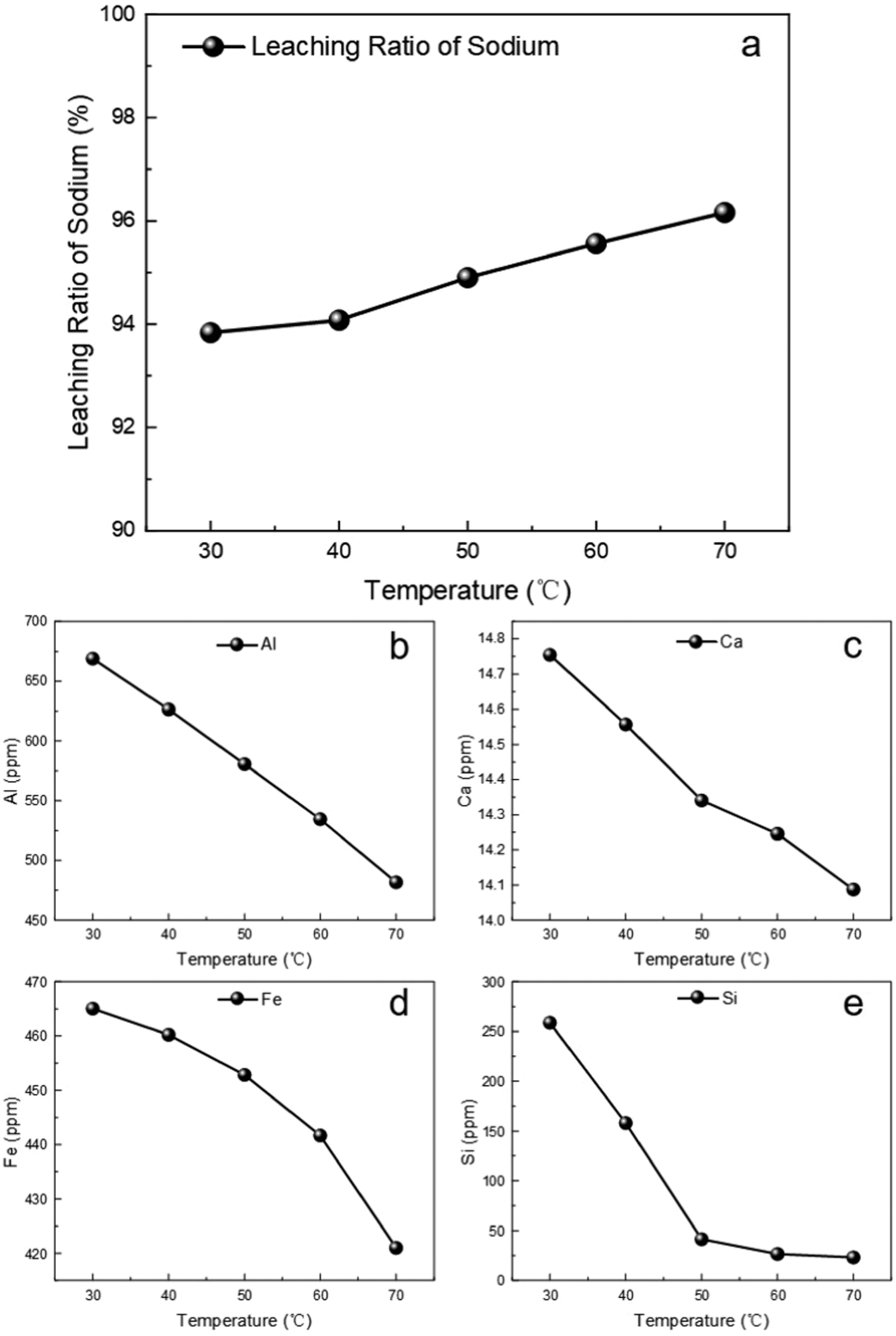

Figure 2. Effect of temperature on the leaching ratio of (a) sodium from RM. The effect of temperature on the concentration of (b) aluminum, (c) calcium, (d) iron, and (e) silicon ions in leaching solution at conditions: 1.2448 mol/L, 120 min, 4/1 (mL/g), and 300 rpm.

$$[Na_6Al_6Si_6O_{24}]\cdot[2NaX \text{ or } Na_2X] \rightleftharpoons 8Na^+ + 6H_4SiO_4 + 6Al(OH)_3 + 8X \quad (X: OH^- \text{ or } CO_3^{2-}) \tag{1}$$

$$Na_6Al_6Si_6O_{24}\cdot 2CaCO_3 + 10H^+ + 16H_2O \rightleftharpoons 6Na^+ + 2Ca^{2+} + 6Al(OH)_3 + 6H_4SiO_4 + 2CO_2\uparrow \tag{2}$$

$$Ca_3Al_2(SiO_4)_x\cdot(OH)_{12-4x} + 6H^+ \rightleftharpoons 3Ca^{2+} + 2Al(OH)_3 + xH_4SiO_4 + (6-4x)H_2O \tag{3}$$

$$Al(OH)_4^- + H^+ \rightleftharpoons Al(OH)_3\downarrow + H_2O \tag{4}$$

$$SiO_3^{2-} + 2H^+ \rightleftharpoons H_2SiO_3\downarrow \tag{5}$$

$$Fe_3^{3+} + 3OH^- \rightleftharpoons Fe(OH)_3\downarrow \tag{6}$$

https://doi.org/10.1021/acsomega.1c04713
ACS Omega 2021, 6, 32798−32808

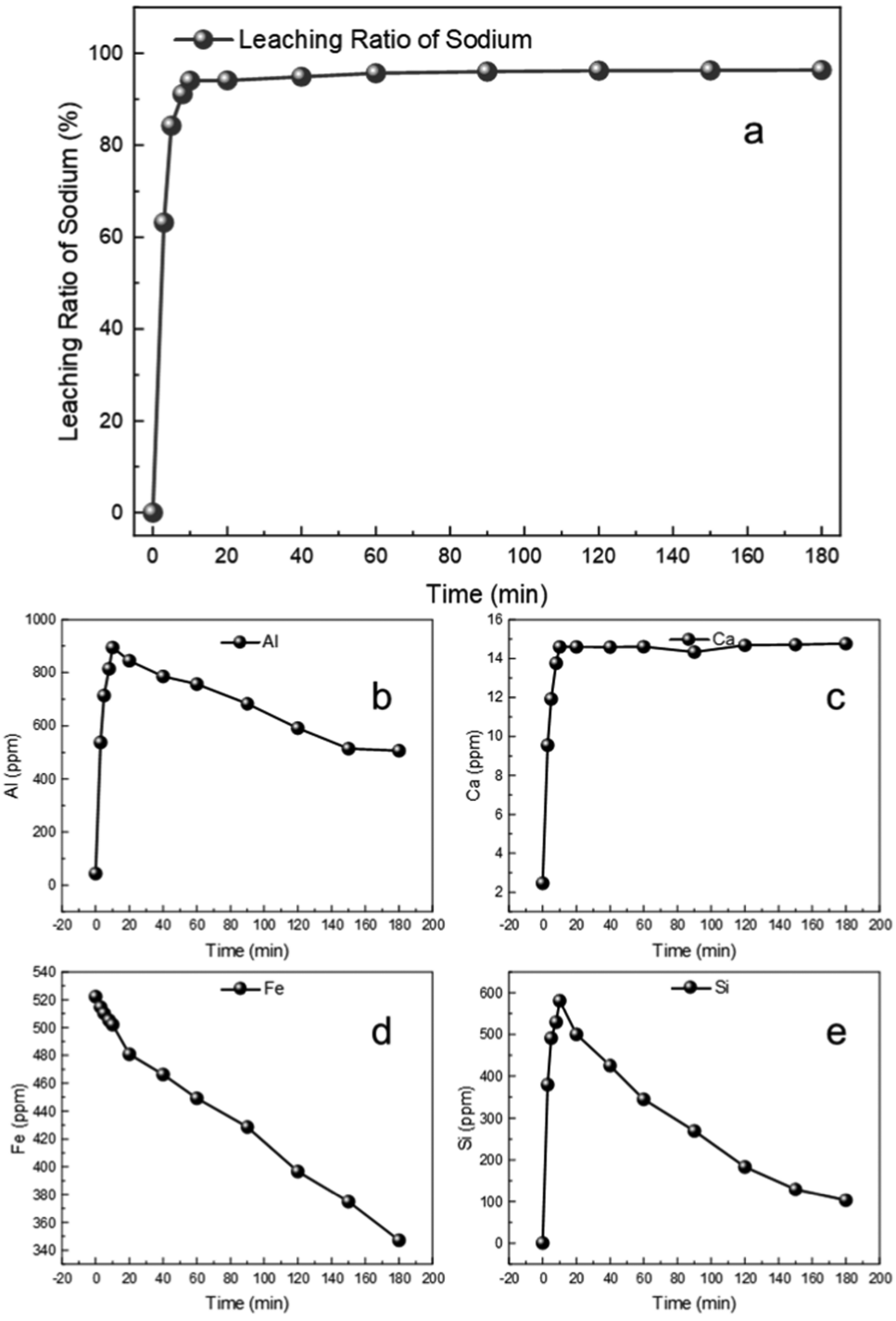

Figure 3. Effect of temperature on the leaching ratio of (a) sodium from RM. The effect of temperature on the concentrations of (b) aluminum, (c) calcium, (d) iron, and (e) silicon ions in the leaching solution at conditions: 1.2448 mol/L, 40 °C, 4/1 (mL/g), and 300 rpm.

$$Ca^{2+} + SO_4^{2-} \rightleftharpoons CaSO_4\downarrow \quad (7)$$

2.2.2. Effect of Acid Leaching Time. Considering the influence of the reaction time, different acid leaching times were used to evaluate the extraction performance of sodium, iron, aluminum, silicon, and calcium ions in RM, as shown in Figure 3. The leaching ratio of sodium rapidly increased to 94.06% in the first 10 min of the experiment, as shown in Figure 3a, which was similar to the report by Zhu et al.[26] The concentrations of aluminum, calcium, and silicon ions also reached the maximum rapidly in the leaching solution 10 min before the experiment. Hematite and most other iron oxides can only be dissolved at a temperature higher than 70 °C when the pH value is less than 1.[45] Therefore, the amount of iron ions leached by hematite and most other iron oxides is low at a lower acid waste acid concentration and lower temperature. The iron ion concentration is higher at the beginning of the dealkalization of RM, almost due to the iron content of waste acid. The hydrogen ion concentration of waste acid continues to decrease, and the iron ion concentration decreases with the increase of alkali reduction time, as shown in Figure 3d, which is related to eq 6.

https://doi.org/10.1021/acsomega.1c04713
ACS Omega 2021, 6, 32798−32808

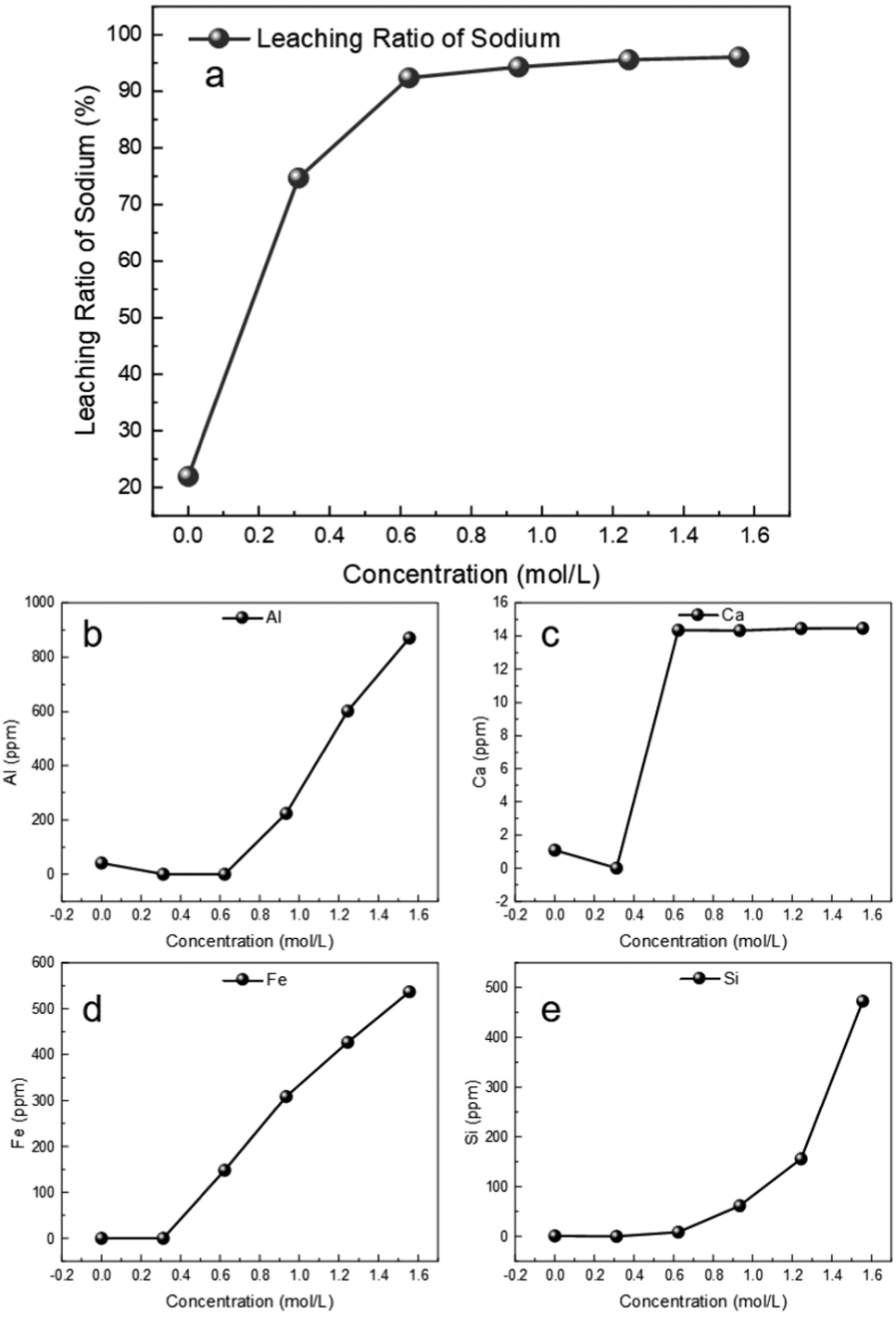

Figure 4. Effect of temperature on the leaching ratio of (a) sodium from RM. The effect of temperature on the concentrations of (b) aluminum, (c) calcium, (d) iron, and (e) silicon ions in the leaching solution at conditions: 120 min, 40 °C, 4/1 (mL/g), and 300 rpm.

At the initial acid leaching stage, RM is mainly controlled by chemical reaction and then controlled by diffusion.[46] The alkali and calcium ions exposed by sodium and calcium ions can react quickly with the acid solution.[47] Therefore, the alkali reduction rate of RM and the concentration of calcium ions in the leaching solution change the fastest within 10 min. Hydrogen ions preferentially react with calcite in RM to form gypsum, and part of calcite reacts with hydrogen ions to release calcium ions (eqs 2 and 3).[48] The solubility product of gypsum remains unchanged. After calcite is wholly transformed into gypsum, the calcium ion concentration remains unchanged (eq 7),[48] so the calcium ion dissolution efficiency remains unchanged. With the progress of the reaction, the sodium and aluminum gradually decrease in RM, which contains insoluble SiO_2/Al_2O_3, forming an inert layer on the surface of RM, which hinders the further leaching of sodium in RM[46] (eqs 4−6). This phenomenon leads to the decrease of the leaching rate and the beginning of the diffusion control step.[46] Therefore, 10 min was selected as the optimal time of the dealkalization of RM in this experiment.

2.2.3. Effect of Acid Concentration. Considering the influence of the acid molar concentration, different concentrations of waste acid were used to evaluate the extraction

https://doi.org/10.1021/acsomega.1c04713
ACS Omega 2021, 6, 32798−32808

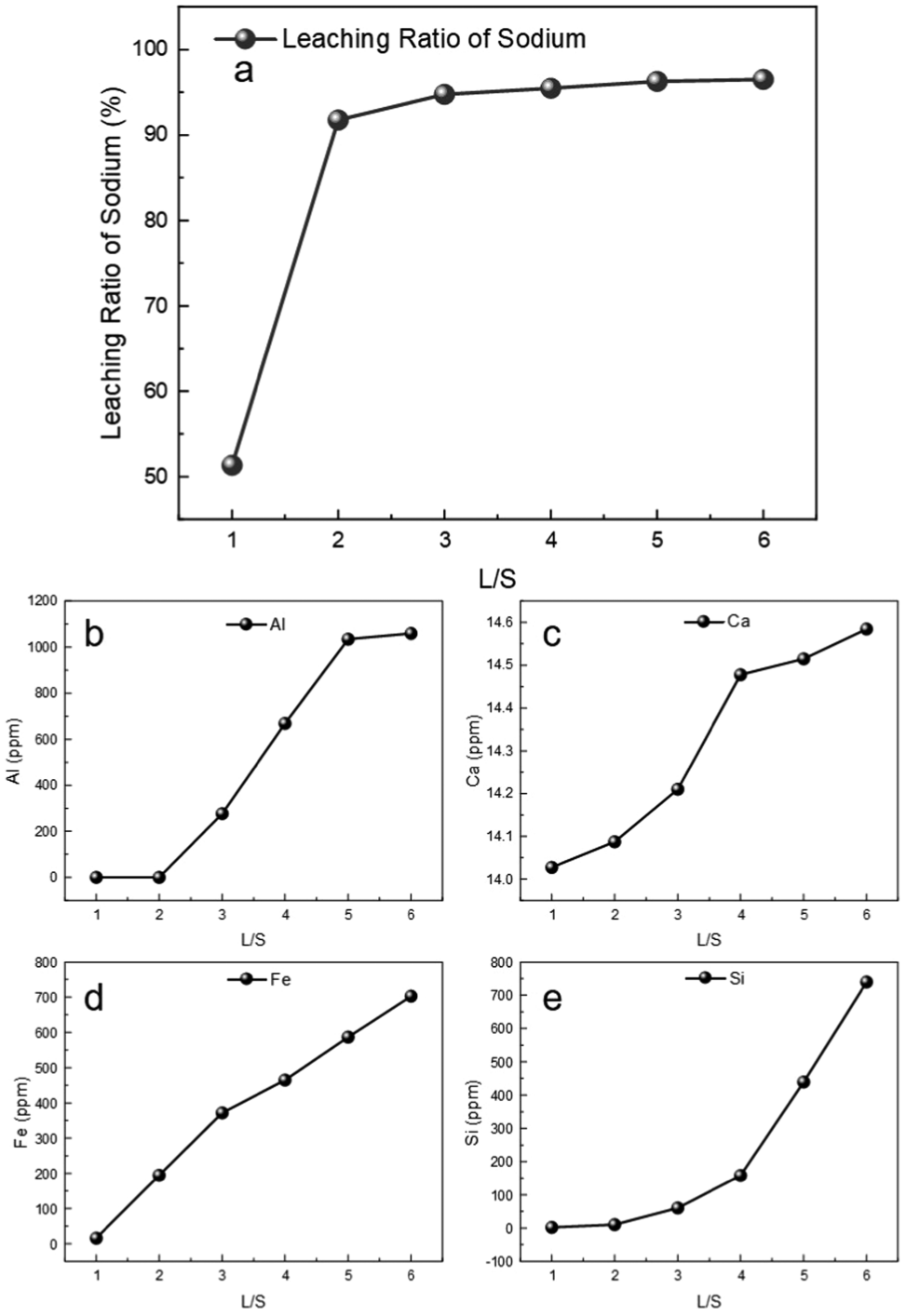

Figure 5. Effect of temperature on the leaching ratio of (a) sodium from RM. The effect of temperature on the concentrations of (b) aluminum, (c) calcium, (d) iron, and (e) silicon ions in leaching solution at conditions: 1.2448 mol/L, 40 °C, 60 min, and 300 rpm.

performance of sodium, iron, aluminum, silicon, and calcium ions in RM, as shown in Figure 4. As shown in Figure 4a, the higher the concentration of waste acid, the better the leaching ratio of sodium. Meanwhile, it can be seen from Figure 4b−e that the leaching amounts of aluminum, calcium, iron, and silicon ions also gradually increase. With the increase in the waste acid concentration to 0.6238 mol/L, the leaching ratio of sodium increased sharply to 92.36%. Before that, the concentration of waste acid was low and first consumed by alkaline substances in RM. At this time, the acid leaching solution was neutral or weakly alkaline, and the solution environment was not conducive to the existence of aluminum, calcium, iron, and silicon ions.[49] With the further increase in waste acid concentration, the higher the hydrogen ion concentration, the more favorable it is for aluminum, iron, and silicon to exist as ions, so their concentrations continue to increase.[50,51] Therefore, 0.6238 mol/L was selected as the optimal acid concentration of the dealkalization of RM in this experiment.

2.2.4. Effect of L/S. Considering the influence of the L/S, different L/S were used to evaluate the extraction performance of sodium, iron, aluminum, silicon, and calcium ions in RM, as

https://doi.org/10.1021/acsomega.1c04713
ACS Omega 2021, 6, 32798−32808

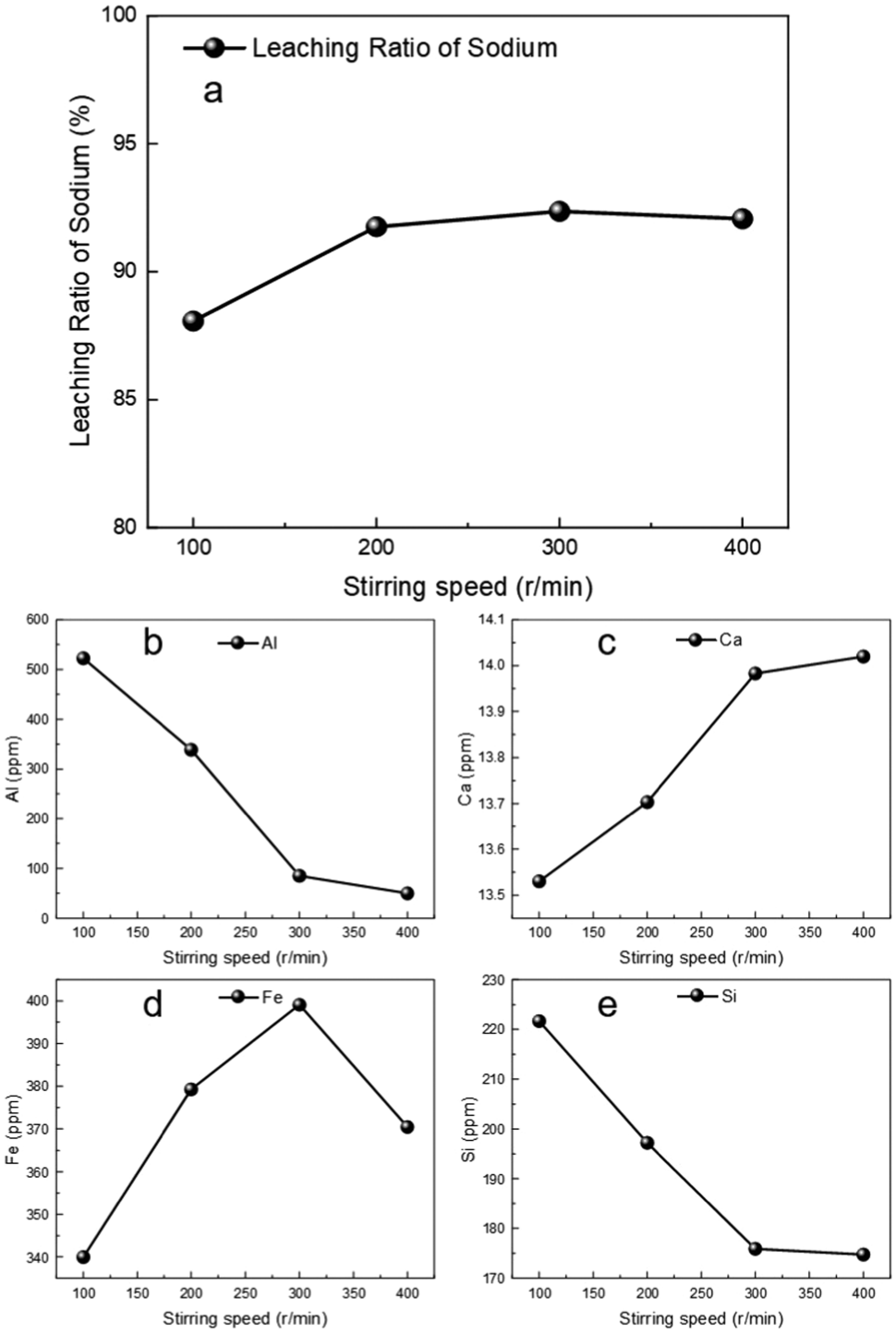

Figure 6. Effect of temperature on the leaching ratio of (a) sodium from RM. The effect of temperature on the concentrations of (b) aluminum, (c) calcium, (d) iron, and (e) silicon ions in the leaching solution at conditions of 0.6238 mol/L, 40 °C, 4/1 (mL/g), and 10 min.

shown in Figure 5. The leaching ratio of sodium is low when the L/S is 1:1, as shown in Figure 5a. When the L/S further increased to 4:1, the leaching ratio of sodium reached 94.76%, but the leaching ratio of sodium did not increase with the further increase of L/S. This is because the L/S directly impacts the slurry viscosity in the system.[52] The larger the L/S, the lower the slurry viscosity and the better the diffusion effect of RM on alkali reduction, which is more conducive to solute diffusion.[52] At the same time, the total amount of waste acid is also relatively high, which is more conducive to the dispersion of aluminum, iron, silicon, and calcium ions in an acid leaching solution under the condition of high L/S. When L/S is low, the reaction system has a large viscosity, and the total amount of waste acid is also relatively low. At this time, the acid in the system is first consumed by the alkaline substance in RM.[49] Therefore, the low L/S condition is not conducive to the dispersion of aluminum, iron, silicon, and calcium ions in the acid leaching solution, and their concentrations are low, as shown in Figure 5b–e. Therefore, 4/1 (mL/g) was selected as the optimal L/S of the dealkalization of RM in this experiment.

https://doi.org/10.1021/acsomega.1c04713
ACS Omega 2021, 6, 32798−32808

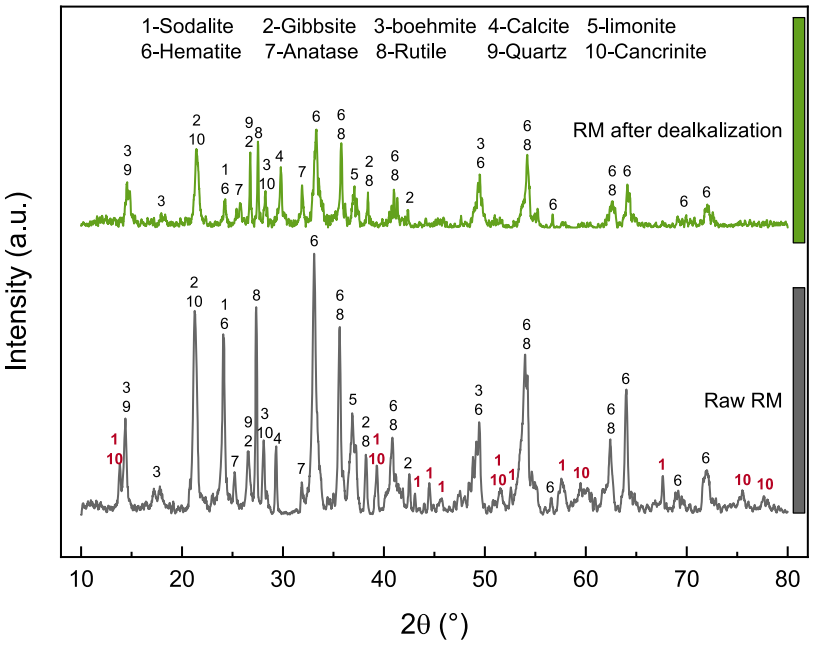

Figure 7. XRD of primary mineral analysis of raw RM and RM after dealkalization.

2.2.5. Effect of Stirring Speed. As shown in Figure 6a, the leaching ratio of sodium was increased from 88.07 to 92.36%, and the stirring speed was increased from 100 to 300 rpm. However, the leaching ratio of sodium decreases when the stirring speed continuously increases. The higher the stirring speed, the greater the centrifugal force, which hinders mass transfer, affects the complete contact between RM and protons, and leads to an incomplete reaction.[20,53] In addition, the higher the stirring speed, the higher the energy consumption. As shown in Figure 6b–e, when the stirring speed increases from 100 to 300 rpm, the dissolution efficiency of aluminum and silicon ions gradually decreases. In contrast, the dissolution efficiency of iron and calcium ions gradually increases. However, when the stirring speed exceeds 300 rpm, the dissolution efficiency of Al, Ca, and Si hardly changes. When the stirring speed exceeds 300 rpm, the iron ion concentration decreases because the increase in the stirring speed increases the centrifugal force, emulsified solution,[20] or co-precipitates with the colloid produced by silicon and aluminum ions.[42,43] Therefore, 300 rpm was selected as the optimal stirring speed in this experiment.

2.3. Phase Analysis. According to X-ray diffractometer (XRD) analysis, the main mineral phases of the raw RM and dealkalized RM (at the optimum conditions of 0.6238 mol/L, 30 °C, 4/1 (mL/g), 300 rpm, and 10 min) are shown in Figure 7. The main mineral phases were sodalite, gibbsite, boehmite, calcite, limonite, cancrinite, anatase, rutile, quartz, and hematite.[54] Sodium mainly exists in sodalite and cancrinite, and it is challenging to remove the bound alkali in RM only by water leaching, which was consistent with other reports.[33] It was found that the mineral phase composition of RM after dealkalization and the raw RM had changed significantly. Most of the structural alkali-bearing substances (sodalite and cancrinite) of RM disappeared. This further confirms the excellent effect of the dealkalization of RM by acid leaching with titanium dioxide waste acid.

3. CONCLUSIONS

Dealkalization is the necessary step for the multipurpose use of RM, and acid leaching is an efficacious method to realize the dealkalization of RM. Most researches focus on recovering metals from the highly alkaline waste by pure acid leaching or stabilization by dealkalization. In this research study, according to the strong alkalinity of RM and strong acidity of titanium dioxide waste acid, RM was leached with titanium dioxide waste acid for dealkalization. The effects of leaching temperature, reaction time, the concentration of waste acid, L/S, and stirring rate on the dealkalization of RM were investigated, and the main elements (aluminum, silicon, iron, calcium) in the dealkalization solution were analyzed. The results show that the leaching ratio of sodium can reach 92.3591% when the leaching temperature is 30 °C, the reaction time is 10 min, the L/S is 4:1, the H_2SO_4 concentration of waste acid is 0.6238 mol/L, and the stirring rate is 300 rpm. Under this condition, the residual alkali content in the RM is 0.2674%, which is a reduction to less than 1%. RM was treated with acid leaching with titanium white waste acid, which could meet the requirements of bulk building materials, consume the waste acid, and realize the reuse of its value by waste control. Compared with the direct use of strong acid leaching for the dealkalization of RM and recovery of precious metals, the cost of dealkalization of RM by waste acid leaching is lower and the treatment speed and capacity are more excellent and more conducive to the healthy development of the alumina industry.

4. MATERIALS AND METHODS

4.1. Samples and Reagents. RM and titanium white waste acid were sampled from an alumina plant and a titanium white powder plant in Chongqing, respectively. The main chemical

Table 1. Main Chemical Composition of RM

composition	Fe_2O_3	Al_2O_3	SiO_2	CaO	TiO_2	Na_2O
mass fraction (wt %)	43.00	23.22	7.77	4.40	4.83	3.50

https://doi.org/10.1021/acsomega.1c04713
ACS Omega 2021, 6, 32798−32808

Table 2. Main Chemical Constituents of Titanium White Waste Acid

composition	H_2SO_4	Fe	Al	total Ti	soluble Ti	Mn	Mg	Ca
content (g/L)	270.05	46.00	2.30	3.90	3.70	1.86	8.02	0.28

Table 3. Parameter Design of Dealkalization of RM with Titanium Dioxide Waste Acid

number	leaching time (min)	temperature (°C)	L/S (mL/g)	acid concentration (mol/L)	stirring speed (rpm)
1	3	40	4	1.2448	300
2	5	40	4	1.2448	300
3	8	40	4	1.2448	300
4	10	40	4	1.2448	300
5	20	40	4	1.2448	300
6	40	40	4	1.2448	300
7	60	40	4	1.2448	300
8	90	40	4	1.2448	300
9	120	40	4	1.2448	300
10	150	40	4	1.2448	300
11	180	40	4	1.2448	300
12	60	40	1	1.2448	300
13	60	40	2	1.2448	300
14	60	40	3	1.2448	300
15	60	40	4	1.2448	300
16	60	40	5	1.2448	300
17	60	40	6	1.2448	300
18	120	30	4	1.2448	300
19	120	40	4	1.2448	300
20	120	50	4	1.2448	300
21	120	60	4	1.2448	300
22	120	70	4	1.2448	300
23	120	40	4	0.0000	300
24	120	40	4	0.3119	300
25	120	40	4	0.6238	300
26	120	40	4	0.9336	300
27	120	40	4	1.2448	300
28	120	40	4	1.5559	300
29	10	40	4	0.6238	100
30	10	40	4	0.6238	200
31	10	40	4	0.6238	300
32	10	40	4	0.6238	400

components were analyzed and detected by ICP-5000 OES/AES (Focused Photonics (Hangzhou), Inc., ICP-5000), and the results are shown in Tables 1 and 2, respectively.

The standard solutions of Na, Al, Ca, Si, and Fe (1000 mg/mL) were purchased from the National Nonferrous Metals and Electronic Materials Analysis and Testing Center of the national standard samples. Distilled water was made by a Pure Water system (Beijing Purkay General Instrument Co., Ltd., GWA-UN2-F40).

4.2. Dealkalization by Acid Leaching. The raw RM was dried in a blast drying oven at 105 °C (SK-101, Shanghai Shengke Instruments & Equipment Co., Ltd.) for 12 h, then ground with a mortar through a 100-mesh sieve, and stored in a sealed bag. The waste acid prepared with a specific concentration was added into a beaker containing 5 g of RM sample at a certain L/S. Then, the RM mixture was heated in a 50 mL beaker under a magnetic stirrer (DF-101S China) at a certain stirring speed, L/S, and reaction temperature for a period of reaction time. The specific experimental design parameters are shown in Table 3.

After the reaction, the mixture was vacuum filtered. Then, the dealkalized RM was dried in a blast drying oven (105 °C, 12 h).

4.3. Analytical Methods. The particle size distribution of the raw RM was determined using a BetterSize 2000 (Dandong Baxter Instrument Ltd) laser particle size analyzer before the screening. ICP-5000 OES/AES was used to analyze the sodium content in RM after alkali removal and the concentration of Al, Si, Ca, and Fe ions in the dealkalization solution. The chemical analysis of Na was performed by a melting method (heating $Li_2B_4O_7/KNO_3$ mixture at 1000 °C for 1 h, followed by dissolving directly in 10% HNO_3 solution).[55] The dissolution efficiency of Na ion (X) is calculated by eq 8

$$X = \left(1 - \frac{M_1}{M_2}\right) \times 100\% \tag{8}$$

where X is the dissolution efficiency of Na ions in %, M_1 is the content of the Na element in the digestion solution of RM after alkali removal in ppm, and M_2 is the content of the Na element in the digestion solution of raw RM in ppm.

The composition of RM after alkali removal was analyzed by an X-ray fluorescence spectrometer (XRF EDX4500H, Skyray Instrument).[53] In addition, the RM samples before and after dealkalization were analyzed by an X-ray diffractometer (XRD-7000, Shimadzu).[54,56] The copper target generated an X-ray with the scanning speed of 5°/min, the scanning angle of 10−80, the tube current of 100 mA, and the tube voltage of 40 kV).

■ ASSOCIATED CONTENT

Supporting Information

The Supporting Information is available free of charge at https://pubs.acs.org/doi/10.1021/acsomega.1c04713.

Particle size distribution table of the original and sifted RM (PDF)

■ AUTHOR INFORMATION

Corresponding Author

Xuejun Quan − *School of Chemistry and Chemical Engineering, Chongqing University of Technology, Chongqing 400054, China*; Email: hengjunq@cqut.edu.cn

Authors

Zhanghao Jiang − *School of Chemistry and Chemical Engineering, Chongqing University of Technology, Chongqing 400054, China*; orcid.org/0000-0002-1263-8998

Shuai Zhao − *School of Chemistry and Chemical Engineering, Chongqing University of Technology, Chongqing 400054, China*

Kui Zeng − *School of Chemistry and Chemical Engineering, Chongqing University of Technology, Chongqing 400054, China*

Hao Chen − *School of Chemistry and Chemical Engineering, Chongqing University of Technology, Chongqing 400054, China*

Yankuo Zhou − *School of Chemistry and Chemical Engineering, Chongqing University of Technology, Chongqing 400054, China*

Complete contact information is available at:

https://pubs.acs.org/10.1021/acsomega.1c04713

Author Contributions

The data that support the findings of this study are available from the corresponding author upon reasonable request.

Notes

The authors declare no competing financial interest.

■ ACKNOWLEDGMENTS

This research was funded by the Postgraduate Innovation Project of Chongqing University of Technology (clgycx 20201006 and clgycx 20203070).

■ ABBREVIATIONS USED

L/S liquid−solid ratio
RM red mud
XRD X-ray diffractometer
XRF X-ray fluorescence

■ REFERENCES

(1) Liang, Y.; Chen, J. Hazards and Utilization of Red Mud. *Pop. Sci. Technol.* **2014**, *16*, 33−34.
(2) Li, R.; Zhang, T.; Liu, Y.; Lv, G.; Xie, L. Calcification-Carbonation Method for Red Mud Processing. *J. Hazard. Mater.* **2016**, *316*, 94−101.
(3) Evans, K. The History, Challenges, and New Developments in the Management and Use of Bauxite Residue. *J. Sustainable Metall.* **2016**, *2*, 316−331.
(4) Fan, D. C.; Ni, W.; Yan, A. Y.; Wang, J. Y.; Cui, W. H. Orthogonal Experiments on Direct Reduction of Carbon-Bearing Pellets of Bayer Red Mud. *J. Iron Steel Res. Int.* **2015**, *22*, 686−693.
(5) Li, Y. W.; Jiang, J.; Xue, S. G.; Millar, G. J.; Kong, X. F.; Li, X. F.; Meng, L. I.; Li, C. X. Effect of Ammonium Chloride on Leaching Behavior of Alkaline Anion and Sodium Ion in Bauxite Residue. *Trans. Nonferrous Met. Soc. China* **2018**, *28*, 2125−2134.
(6) Liu, W.; Chen, X.; Li, W.; Yu, Y.; Yan, K. Environmental Assessment, Management and Utilization of Red Mud in China. *J. Cleaner Prod.* **2014**, *84*, 606−610.
(7) Samal, S.; Ray, A. K.; Bandopadhyay, A. Proposal for Resources, Utilization and Processes of Red Mud in India—A Review. *Int. J. Miner. Process.* **2013**, *118*, 43−55.
(8) Xue, S.; Kong, X.; Zhu, F.; Hartley, W.; Li, X.; Li, Y. Proposal for Management and Alkalinity Transformation of Bauxite Residue in China. *Environ. Sci. Pollut. Res.* **2016**, *23*, 12822−12834.
(9) Power, G.; Gräfe, M.; Klauber, C. Bauxite Residue Issues: I. Current Management, Disposal and Storage Practices. *Hydrometallurgy* **2011**, *108*, 33−45.
(10) Li, X. B.; Wei, X. I. A. O.; Wei, L. I. U.; Liu, G. H.; Peng, Z. H.; Zhou, Q. S.; Qi, T. G. Recovery of Alumina and Ferric Oxide from Bayer Red Mud Rich in Iron by Reduction Sintering. *Trans. Nonferrous Met. Soc. China* **2009**, *19*, 1342−1347.
(11) Mukiza, E.; Zhang, L. L.; Liu, X.; Zhang, N. Utilization of Red Mud in Road Base and Subgrade Materials: A Review. *Resour., Conserv. Recycl.* **2019**, *141*, 187−199.
(12) Ghosh, I.; Guha, S.; Balasubramaniam, R.; Kumar, A. V. R. Leaching of Metals from Fresh and Sintered Red Mud. *J. Hazard. Mater.* **2011**, *185*, 662−668.
(13) Rubinos, D. A.; Barral, M. T. Fractionation and Mobility of Metals in Bauxite Red Mud. *Environ. Sci. Pollut. Res.* **2013**, *20*, 7787−7802.
(14) Zhu, F.; Li, X.; Xue, S.; Hartley, W.; Wu, C.; Han, F. Natural Plant Colonization Improves the Physical Condition of Bauxite Residue over Time. *Environ. Sci. Pollut. Res.* **2016**, *23*, 22897−22905.
(15) Liu, W.; Yang, J.; Xiao, B. Application of Bayer Red Mud for Iron Recovery and Building Material Production from Alumosilicate Residues. *J. Hazard. Mater.* **2009**, *161*, 474−478.
(16) Zhu, F.; Li, Y.; Xue, S.; Hartley, W.; Wu, H. Effects of Iron-Aluminium Oxides and Organic Carbon on Aggregate Stability of Bauxite Residues. *Environ. Sci. Pollut. Res.* **2016**, *23*, 9073−9081.
(17) Wang, X.; Sun, T.; Wu, S.; Chen, C.; Kou, J.; Xu, C. A Novel Utilization of Bayer Red Mud through Co-Reduction with a Limonitic Laterite Ore to Prepare Ferronickel. *J. Cleaner Prod.* **2019**, *216*, 33−41.
(18) Lyu, F.; Sun, N.; Sun, W.; Khoso, S. A.; Tang, H. H.; Wang, L. Preliminary Assessment of Revegetation Potential through Ryegrass Growing on Bauxite Residue. *J. Cent. South Univ.* **2019**, *26*, 404−409.
(19) Klauber, C.; Harwood, N.; Hockridge, R.; Middleton, C. Proposed Mechanism for the Formation of Dust Horizons on Bauxite Residue Disposal Areas. In *Essential Readings in Light Metals*; Springer: Cham, 2017.
(20) Kong, X.; Li, M.; Xue, S.; Hartley, W.; Chen, C.; Wu, C.; Li, X.; Li, Y. Acid Transformation of Bauxite Residue: Conversion of Its Alkaline Characteristics. *J. Hazard. Mater.* **2017**, *324*, 382−390.
(21) Yi, R. R.; Cao, W. Current Situation and Prospect of Comprehensive Utilization of Red Mud. *Appl. Mech. Mater.* **2014**, *522*−*524*, 811−816.
(22) Davris, P.; Balomenos, E.; Panias, D.; Paspaliaris, I. Selective Leaching of Rare Earth Elements from Bauxite Residue (Red Mud), Using a Functionalized Hydrophobic Ionic Liquid. *Hydrometallurgy* **2016**, *164*, 125−135.
(23) He, H.; Yue, Q.; Qi, Y.; Gao, B.; Zhao, Y.; Yu, H.; Li, J.; Li, Q.; Wang, Y. The Effect of Incorporation of Red Mud on the Properties of Clay Ceramic Bodies. *Appl. Clay Sci.* **2012**, *70*, 67−73.
(24) Kang, S. P.; Kwon, S. J. Effects of Red Mud and Alkali-Activated Slag Cement on Efflorescence in Cement Mortar. *Constr. Build. Mater.* **2017**, *133*, 459−467.
(25) Topličić-Ćurčić, G.; Mitic, V.; Grdić, D.; Ristić, N.; Grdić, Z. In *Environmental Aspects of Red Mud and Its Utilization as a Component of Building Materials*, Proceedings of the IV Advanced Ceramics and Applications Conference; Atlantis Press: Paris, 2017; pp 447−474.
(26) Zhu, X.; Li, W.; Guan, X. An Active Dealkalization of Red Mud with Roasting and Water Leaching. *J. Hazard. Mater.* **2015**, *286*, 85−91.
(27) Chen, L.; Bin; Zhang, Y. F.; Zhang, Y. Dealkalization of Red Mud Generated in Alumina Production by Sub-Molten Salt Process under Atmospheric Pressure. *Chin. J. Process Eng.* **2010**, *10*, 470−475.
(28) Liu, Z.; Li, H.; Huang, M.; Jia, D.; Zhang, N. Effects of Cooling Method on Removal of Sodium from Active Roasting Red Mud Based on Water Leaching. *Hydrometallurgy* **2017**, *167*, 92−100.
(29) Luo, M.; Qi, X.; Zhang, Y.; Ren, Y.; Tong, J.; Chen, Z.; Hou, Y.; Yeerkebai, N.; Wang, H.; Feng, S.; Li, F. Study on Dealkalization and Settling Performance of Red Mud. *Environ. Sci. Pollut. Res.* **2017**, *24*, 1794−1802.
(30) Wei, G.; Shao, L.; Mo, J.; Li, Z.; Zhang, L. Preparation of a New Fenton-like Catalyst from Red Mud Using Molasses Wastewater as Partial Acidifying Agent. *Environ. Sci. Pollut. Res.* **2017**, *24*, 15067−15077.
(31) Huang, Y.; Chai, W.; Han, G.; Wang, W.; Yang, S.; Liu, J. A Perspective of Stepwise Utilisation of Bayer Red Mud: Step Two-Extracting and Recovering Ti from Ti-Enriched Tailing with Acid Leaching and Precipitate Flotation. *J. Hazard. Mater.* **2016**, *307*, 318−327.
(32) Jin, J.; Liu, L.; Liu, R.; Wei, H.; Qian, G.; Zheng, J.; Xie, W.; Lin, F.; Xie, J. Preparation and Thermal Performance of Binary Fatty Acid with Diatomite as Form-Stable Composite Phase Change Material for Cooling Asphalt Pavements. *Constr. Build. Mater* **2019**, *226*, 616−624.
(33) Wang, Y.; Zhang, T. an.; Lyu, G.; Guo, F.; Zhang, W.; Zhang, Y. Recovery of Alkali and Alumina from Bauxite Residue (Red Mud) and Complete Reuse of the Treated Residue. *J. Cleaner Prod.* **2018**, *188*, 456−465.
(34) Freire, T. S. S.; Clark, M. W.; Comarmond, M. J.; Payne, T. E.; Reichelt-Brushett, A. J.; Thorogood, G. J. Electroacoustic Isoelectric Point Determinations of Bauxite Refinery Residues: Different Neutralization Techniques and Minor Mineral Effects. *Langmuir* **2012**, *28*, 11802−11811.

(35) Chen, H.; Wang, T.; Yang, K.; Shengbi, W. Technology Conditions and Mechanism Discussion of Sodium and Iron Extraction from Red Mud by Acid. *Inorg. Chem. Ind.* **2016**, *48*, 44−48.
(36) Onay, O. Influence of Pyrolysis Temperature and Heating Rate on the Production of Bio-Oil and Char from Safflower Seed by Pyrolysis, Using a Well-Swept Fixed-Bed Reactor. *Fuel Process. Technol.* **2007**, *88*, 523−531.
(37) Tuncuk, A.; Ciftlik, S.; Akcil, A. Factorial Experiments for Iron Removal from Kaolin by Using Single and Two-Step Leaching with Sulfuric Acid. *Hydrometallurgy* **2013**, *134−135*, 80−86.
(38) Borra, C. R.; Blanpain, B.; Pontikes, Y.; Binnemans, K.; Van Gerven, T. Recovery of Rare Earths and Major Metals from Bauxite Residue (Red Mud) by Alkali Roasting, Smelting, and Leaching. *J. Sustainable Metall.* **2017**, *3*, 393−404.
(39) Rao, B. H.; Reddy, N. G. Zeta Potential and Particle Size Characteristics of Red Mud Waste. In *Geoenvironmental Practices and Sustainability*; Springer, 2017; pp 69−89.
(40) Lu, R.; Zhang, Y.; Zhou, F.; Wang, X. Research of Leaching Alumina and Iron Oxide from Bayer Red Mud. *Appl. Mech. Mater.* **2012**, *151*, 355−359.
(41) Wang, C.; Zhang, X.; Sun, R.; Cao, Y. Neutralization of Red Mud Using Bio-Acid Generated by Hydrothermal Carbonization of Waste Biomass for Potential Soil Application. *J. Cleaner Prod.* **2020**, *271*, No. 122525.
(42) Man, K.; Zhu, Q.; Li, L.; Liu, C.; Xing, Z. Preparation and Performance of Ceramic Filter Material by Recovered Silicon Dioxide as Major Leached Component from Red Mud. *Ceram. Int.* **2017**, *43*, 7565−7572.
(43) Zhang, J. J.; Deng, Z. G.; Xu, T. H. Experimental Investigation on Leaching Metals from Red Mud. *Light Met.* **2005**, *2*, 13−15.
(44) Kirwan, L. J.; Hartshorn, A.; McMonagle, J. B.; Fleming, L.; Funnell, D. Chemistry of Bauxite Residue Neutralisation and Aspects to Implementation. *Int. J. Miner. Process.* **2013**, *119*, 40−50.
(45) Pepper, R. A.; Couperthwaite, S. J.; Millar, G. J. Comprehensive Examination of Acid Leaching Behaviour of Mineral Phases from Red Mud: Recovery of Fe, Al, Ti, and Si. *Miner. Eng.* **2016**, *99*, 8−18.
(46) Kashefi, K.; Pardakhti, A.; Shafiepour, M.; Hemmati, A. Process Optimization for Integrated Mineralization of Carbon Dioxide and Metal Recovery of Red Mud. *J. Environ. Chem. Eng.* **2020**, *8*, No. 103638.
(47) Hu, G.; Lyu, F.; Khoso, S. A.; Zeng, H.; Sun, W.; Tang, H.; Wang, L. Staged Leaching Behavior of Red Mud during Dealkalization with Mild Acid. *Hydrometallurgy* **2020**, *196*, No. 105422.
(48) Wang, L.; Ji, B.; Hu, Y.; Liu, R.; Sun, W. A Review on in Situ Phytoremediation of Mine Tailings. *Chemosphere* **2017**, *184*, 594−600.
(49) Liang, W.; Couperthwaite, S. J.; Kaur, G.; Yan, C.; Johnstone, D. W.; Millar, G. J. Effect of Strong Acids on Red Mud Structural and Fluoride Adsorption Properties. *J. Colloid Interface Sci.* **2014**, *423*, 158−165.
(50) Agatzini-Leonardou, S.; Oustadakis, P.; Tsakiridis, P. E.; Markopoulos, C. Titanium Leaching from Red Mud by Diluted Sulfuric Acid at Atmospheric Pressure. *J. Hazard. Mater.* **2008**, *157*, 579−586.
(51) Burstein, G. T. The Iron Oxides: Structure, Properties, Reactions, Occurrence and Uses. *Corros. Sci.* **1997**, *39*, 1499−1500.
(52) Borra, C. R.; Pontikes, Y.; Binnemans, K.; Van Gerven, T. Leaching of Rare Earths from Bauxite Residue (Red Mud). *Miner. Eng.* **2015**, *76*, 20−27.
(53) Zhang, Y.; Hu, Y.; Sun, N.; Khoso, S. A.; Wang, L.; Sun, W. A Novel Precipitant for Separating Lithium from Magnesium in High Mg/Li Ratio Brine. *Hydrometallurgy* **2019**, *187*, 125−133.
(54) Xue, S. G.; Wu, Y. J.; Li, Y. W.; Chuan, W. U.; Kong, X. F.; Zhu, F.; William, H.; Li, X. F.; Ye, Y. Z. Industrial Wastes Applications for Alkalinity Regulation in Bauxite Residue: A Comprehensive Review. *J. Cent. South Univ.* **2019**, *26*, 268−288.
(55) Keller, V.; Stopic, S.; Xakalashe, B.; Ma, Y.; Ndlovu, S.; Mwewa, B.; Simate, G. S.; Friedrich, B. Effectiveness of Fly Ash and Red Mud as Strategies for Sustainable Acid Mine Drainage Management. *Minerals* **2020**, *10*, No. 707.
(56) Cadena, E. Microscopical and Elemental FESEM and Phenom ProX-SEM-EDS Analysis of Osteocyte- and Blood Vessel-like Microstructures Obtained from Fossil Vertebrates of the Eocene Messel Pit, Germany. *PeerJ* **2016**, *2016*, No. e1618.

https://doi.org/10.1021/acsomega.1c04713
ACS Omega 2021, 6, 32798−32808